

## **Pathogen exposure misclassification can bias association signals in GWAS of infectious diseases when using population-based common controls**

Dylan Duchon,<sup>1</sup> Candelaria Vergara,<sup>1</sup> Chloe L. Thio,<sup>2</sup> Prosenjit Kundu,<sup>3</sup> Nilanjan Chatterjee,<sup>3</sup>

David L. Thomas,<sup>2</sup> Genevieve L. Wojcik,<sup>†1</sup> Priya Duggal<sup>†\*1</sup>

<sup>1</sup> Department of Epidemiology, Johns Hopkins Bloomberg School of Public Health, Baltimore, MD, 21205, USA

<sup>2</sup> Division of Infectious Diseases, Johns Hopkins School of Medicine, Baltimore, MD, 21205, USA

<sup>3</sup> Department of Biostatistics, Johns Hopkins Bloomberg School of Public Health, Baltimore, MD, 21205, USA

†These senior authors contributed equally

\*Correspondence: [pduggal@ihj.edu](mailto:pduggal@ihj.edu)

NOTE: This preprint reports new research that has not been certified by peer review and should not be used to guide clinical practice.

1 **ABSTRACT**

2 Genome-wide association studies (GWAS) have been performed to identify host genetic factors  
3 for a range of phenotypes, including for infectious diseases. The use of population-based  
4 common controls from biobanks and extensive consortiums is a valuable resource to increase  
5 sample sizes in the identification of associated loci with minimal additional expense. Non-  
6 differential misclassification of the outcome has been reported when the controls are not well-  
7 characterized, which often attenuates the true effect size. However, for infectious diseases the  
8 comparison of cases to population-based common controls regardless of pathogen exposure  
9 can also result in selection bias. Through simulated comparisons of pathogen exposed cases  
10 and population-based common controls, we demonstrate that not accounting for pathogen  
11 exposure can result in biased effect estimates and spurious genome-wide significant signals.  
12 Further, the observed association can be distorted depending upon strength of the association  
13 between a locus and pathogen exposure and the prevalence of pathogen exposure. We also  
14 used a real data example from the hepatitis C virus (HCV) genetic consortium comparing HCV  
15 spontaneous clearance to persistent infection with both well characterized controls, and  
16 population-based common controls from the UK Biobank. We find biased effect estimates for  
17 known HCV clearance-associated loci and potentially spurious HCV clearance-associations.  
18 These findings suggest that the choice of controls is especially important for infectious diseases  
19 or outcomes that are conditional upon environmental exposures.

## 20 **INTRODUCTION**

21 Genome-wide association studies (GWAS) are focused on identifying genetic associations with  
22 health outcomes. This has been successfully accomplished using well-characterized cases and  
23 controls often from epidemiologic cohort or case-control studies.<sup>1</sup> More recently, GWAS have  
24 utilized biobanks and consortiums to expand sample populations. This can include comparing  
25 well-characterized cases to phenotypically uncharacterized or population-based common  
26 controls which has led to the identification of novel associations with low to modest effect size  
27 s.<sup>2-9</sup> Concerns related to the use of common controls include not adequately accounting for  
28 population substructure and the likelihood of non-differential misclassification across the  
29 outcome (i.e. some proportion of the controls have developed the outcome of interest) which  
30 can often attenuate true associations.<sup>2,6,8-10</sup>

31 When studying infectious disease, it is key that an individual is exposed to a pathogen (i.e.  
32 virus, bacteria, protozoa) before they can develop disease. Host genetics and immunity along  
33 with pathogen genetics, co-infections, co-morbidities, age, and sex are known to explain some  
34 of the heterogeneity in disease outcomes. Thus, it is critical to account for pathogen exposure  
35 because unexposed individuals are never at risk of developing the outcome. This can be  
36 achieved through antibody or antigen testing or obtaining documented history of exposure (i.e.  
37 vaccine, contact tracing). While it is assumed that the internal validity of case-control studies,  
38 including GWAS, is maintained by the characterization of both the genetic exposure and the  
39 phenotypic outcome for every study participant, it is also assumed that cases and controls are  
40 at risk of developing the outcome. For infectious disease studies involving population-based  
41 common controls, this presumption is not always true and can result in differential  
42 misclassification of pathogen exposure between cases and controls.<sup>11,12</sup> Whether  
43 epidemiological factors that influence pathogen exposure (i.e. increased transmission in certain

44 populations or occupations, routes of transmission, or comorbidities) can subsequently result in  
45 spurious genetic association signals due to this misclassification is not fully explored.

46 In this study, we performed simulations comparing cases to well-characterized controls with  
47 known exposures and to population-based common controls with unknown exposures to identify  
48 if external variables associated with pathogen exposure can induce spurious associations. We  
49 also used empirical data to compare the genetic association results from a GWAS performed to  
50 identify host loci associated with recovery from hepatitis C virus (HCV) infection using either  
51 known HCV-exposed and persistently infected controls or population-based common controls  
52 from the UK Biobank (UKB).

## 53 **SUBJECTS AND METHODS**

### 54 **Simulations to characterize pathogen exposure-associated selection bias**

55 The directed acyclic graph (DAG) depicted in **Figure 1** provides a graphical representation of  
56 how comparing exposed cases to population-based common controls differs from comparisons  
57 made to well-characterized (pathogen-exposed) controls. For loci associated with pathogen  
58 exposure (e.g., a causal locus for a risk factor of pathogen exposure) unrelated to the outcome  
59 of interest, if unequivocally pathogen exposed cases are compared to population-based  
60 common controls regardless of exposure status, differential misclassification of pathogen  
61 exposure can induce selection bias, resulting in spurious associations between the outcome  
62 and the loci associated with pathogen exposure.

63 How strongly pathogen exposure is associated with case status determines the strength of this  
64 bias (i.e., the dashed red line reflecting the degree of differential misclassification in pathogen  
65 exposure in **Figure 1**). Simulations were performed to assess whether the association between  
66 a non-outcome associated SNP can become spuriously associated with the outcome due to a  
67 relationship with pathogen exposure. Whether the prevalence of a pathogen contributes to this  
68 bias was also determined by assessing the degree to which inflated effect estimates for the

69 outcome~SNP relationship were observed across the various simulation scenarios. Simulations  
70 were performed using the lavaan package (v0.6-8) in R as it allows for the control of statistical  
71 associations between simulated variables.<sup>13,14</sup> The phenotypic data and SNP genotypes were  
72 simulated for a large cohort (N=1,000,000).

73 Case and control definitions: **Cases** were defined as individuals with a known pathogen  
74 exposure who developed the clinical outcome. '**Well-characterized controls**' were defined as  
75 individuals with a known pathogen exposure event but did not develop the clinical outcome. To  
76 investigate the effects of differential misclassification of pathogen exposure in the absence of  
77 non-differential misclassification of the outcome, '**population-based common controls**' were  
78 defined as any individual who did not develop the clinical outcome, regardless of pathogen  
79 exposure. In each simulated cohort, a fixed number of cases, well-characterized controls, and  
80 population-based common controls were randomly sampled from individuals meeting the  
81 inclusion criteria. In each simulated cohort, unless otherwise stated, the prevalence of pathogen  
82 exposure was set at 25%. Cases were selected from the exposed population, of which 50% had  
83 the observed clinical outcome and the remainder defined as well-characterized controls. As  
84 population-based common controls were selected from the entire population, excluding cases, a  
85 proportion of the population-based controls would be expected to have a simulated pathogen  
86 exposure.

87 Simulated variables: Additional simulated variables included a single nucleotide polymorphism  
88 (SNP, coded as 0,1, 2 minor alleles) and a variable associated with pathogen exposure (U1  
89 which could represent routes of transmission, occupation, comorbidities, etc.). To explore the  
90 effect of confounding within a locus completely unrelated the outcome of interest, neither the  
91 SNP nor the U1 variable were simulated to be associated with the outcome. For all simulated  
92 cohorts, the SNP had a fixed minor allele frequency (MAF) of 15% and a fixed SNP~U1  
93 association ( $\beta$ ) of 0.1, whereby each additional SNP allele was associated with an increase of

94 10% of U1. Similar effect sizes have been observed for markers associated with other complex  
95 diseases.<sup>15–19</sup> The SNP was simulated with a MAF of 15% and in Hardy Weinberg Equilibrium  
96 (HWE). The effect estimates for associations between simulated variables were confirmed via  
97 logistic and linear model-based regressions using the speedglm package in R.<sup>13,14</sup>

98 Simulation scenario 1 – Effects of a pathogen exposure-specific variable: We simulated 500,000  
99 replicates of N=1,000,000 individuals for each of the following relationships between U1 and  
100 pathogen exposure: no association ( $\beta=0$ , OR=1), a moderate association ( $\beta=\log(1.2)$ , OR=1.2),  
101 or a strong association ( $\beta=\log(2)$ , OR=2). Simulations were performed assuming the prevalence  
102 of pathogen exposure was 25% and 50% of exposed individuals had the outcome (**Table 1**).

103 Simulation scenario 2 – Effects of the prevalence of pathogen exposure: We simulated 500,000  
104 replicates of N=1,000,000 individuals for each of the following pathogen exposure prevalences:  
105 5%, 25%, 50%, 75%, or 100%. Simulations were performed assuming either a moderate  
106 ( $\beta=\log(1.2)$ , OR=1.2) or a strong association ( $\beta=\log(2)$ , OR=2) between U1 and pathogen  
107 exposure and 50% of exposed individuals had the outcome (**Table 1**).

108 Simulated genetic associations:

109 In each simulated replicate, 20,000 cases, 20,000 well-characterized controls, and 20,000  
110 population-based controls were randomly selected and included in logistic regressions to  
111 quantify the ‘outcome of interest’~SNP association. Regressions compared cases to population-  
112 based controls (scenarios 1a and 2a) or well-characterized controls (scenarios 1b and 2b). To  
113 simulate a realistic use-case of GWAS involving many common controls, we re-performed the  
114 above simulations and regressions for both scenarios comparing 20,000 cases to 200,000  
115 population-based controls. Regressions were performed in R using the Rfast package.<sup>20</sup>

116 To test whether the effect sizes of the SNP~outcome associations ( $\beta_{\text{SNP}}$ ) were significantly  
117 different when cases were compared to population-based or well-characterized controls, we  
118 derived a modified Z statistic, appropriate for the comparison of regression coefficients,<sup>21</sup>

119 reflecting the change in average scenario-specific beta estimates for each parameter between  
120 comparisons involving population-based controls and well-characterized controls. The standard  
121 error term used to estimate each Z score was defined as the mean standard error across each  
122 scenario's parameter-specific set of simulations. This conservative test was chosen due to the  
123 extreme number of comparisons (e.g., with two logistic regressions for each of the parameter-  
124 specific 500,000 replicates, 13 million regressions were performed when comparing 20,000  
125 cases to 20,000 population-based controls).

126 As a null association for the 'outcome of interest'~SNP relationship was simulated for each  
127 cohort, any non-null observed 'outcome of interest'~SNP association reflect spurious signals  
128 induced via the scenario-specific selection of case and controls. We calculated the proportion of  
129 cohorts with 'outcome of interest'~SNP associations that reached the conservative but widely  
130 accepted genome-wide significance threshold of  $P \leq 5 \times 10^{-8}$ .<sup>22</sup> To determine whether the  
131 prevalence of pathogen exposure was associated with the magnitude of these spurious signals,  
132 we performed linear regressions to obtain the magnitude and direction of the average beta  
133 estimates obtained from each set of pathogen exposure prevalence parameter-specific  
134 simulations. Measures of heterogeneity were estimated using the meta R package for each set  
135 of parameter-specific simulations to confirm independent yet equivalent cohorts were simulated  
136 (**Table S1**).<sup>23</sup> Additional simulations were considered and are included in the supplementary  
137 methods.

### 138 **HCV GWAS using cases and well characterized controls or population-based controls**

#### 139 *Well characterized cases and controls from the HCV Extended Genetics Consortium*

140 We leveraged data from The HCV Extended Genetic Consortium (HCV Consortium) which  
141 includes 1,869 individuals of African ancestry, 1,739 individuals of European ancestry, and 486  
142 individuals of Hispanic ancestry who passed GWAS-related quality control metrics,<sup>24</sup> as  
143 previously described.<sup>25-27</sup> We only used individuals of European ancestry in this study (tightly

144 clustered with the 1000 Genomes Project (1000G) Northern European population from Utah  
145 (CEU) and had an admixture estimate of at least 90% European ancestry, determined via  
146 fastSTRUCTURE).<sup>28</sup> Of the 1,739 European ancestry HCV consortium individuals, 702 were  
147 individuals with serological evidence of spontaneous clearance from HCV infection (cases) and  
148 1,037 were defined as individuals with persistent HCV infection (“well-characterized controls”).<sup>25</sup>  
149 Of these individuals, 16% were living with HIV and 31% were female.<sup>25–27</sup>

150 The UK Biobank (UKB) is a large population-level cohort including 500,000 volunteers recruited  
151 from across the UK.<sup>29</sup> ‘Population-based controls’ were unrelated individuals from the UKB who  
152 were identified to be of similar genetic ancestry to HCV Consortium individuals of European  
153 ancestry. For these individuals, we had no information on HCV infection status or previous  
154 exposure to HCV.

#### 155 Selection of samples for analysis

156 Ancestry analysis of the combined HCV Consortium-UKB cohort: Linkage disequilibrium (LD)-  
157 based pruning was used to iteratively remove variants in LD ( $r^2 > 0.2$ ) via a sliding 500k base-  
158 pair-wide window prior to performing principal components analysis (PCA) in the combined HCV  
159 Consortium-UKB cohort. This LD-based pruning was performed on all genetic markers with  
160 missingness  $< 1.5\%$  and MAF  $> 2.5\%$ , after excluding regions of long-range linkage  
161 disequilibrium.<sup>30</sup> Given the extreme sample size of the combined HCV-UKB cohorts, FastPCA  
162 was used.<sup>31,32</sup> LD-based pruning and PCA was carried out using the R package SNPRelate.<sup>33</sup>

163 Selection of ancestry-matched UKB population-based controls: Out of 487,409 UKB individuals  
164 with genetic data available, 407,192 UKB participants who passed previously described QC  
165 metrics were included within our analyses.<sup>29,34,35</sup> We limited UKB population-based controls to  
166 370,702 ancestry-matched individuals genetically similar to the European individuals from the  
167 HCV Consortium (**Figures S1-S2**).<sup>36</sup> Briefly, genetic ancestry-based matching of cases and  
168 controls was accomplished through multiple iterations of PCA. Initially, the UKB participants



169 whose top three PCs were within six standard deviations of the mean PC values estimated from  
170 HCV Consortium individuals were retained for analysis (N=383,724). A second PCA filtering  
171 step, using the top twenty PCs, excluded any UKB individual with estimated eigenvalues 5%  
172 higher or lower than the range of PC-specific values from HCV Consortium individuals. A total of  
173 370,702 ancestry-matched UKB controls were identified.

#### 174 Selection of markers for analysis

175 HCV Consortium: Out of an initial 661,397 directly genotyped markers mapped to the  
176 GRCh37/hg19 reference sequence, a total of 656,340 markers had MAF >1%, variant-level call  
177 rates >97%, were in Hardy-Weinberg Equilibrium (HWE) based on HWE exact tests ( $P > 1 \times 10^{-5}$ ),  
178 and passed the ‘McCarthy Group Tools’ Haplotype Reference Consortium (HRC) imputation  
179 preparation pipeline (<https://www.well.ox.ac.uk/~wrayner/tools/>).<sup>37</sup> No allele frequency difference  
180 threshold between this database and the HCV Consortium cohort individuals was used to  
181 remove genotyped markers. Imputation was performed using the HRC (version r1.1, 2016)  
182 European reference panel via the Michigan Imputation Server and phased using Eagle  
183 (v2.4).<sup>38,39</sup> Markers with imputation quality  $R^2$  values > 0.3 were retained and markers which  
184 were not bi-allelic or had a genotyping rate < 97% or MAF < 1% were removed. Additionally,  
185 imputed markers with variant-level INFO scores <90% or HWE  $P < 5 \times 10^{-7}$  were removed. A total  
186 of 6,468,618 imputed markers passed these QC metrics.

187 UK Biobank: A total of 670,739 directly genotyped autosomal QC-passed markers were used for  
188 imputation, as previously described.<sup>29</sup> Phasing was performed with SHAPEIT3 and imputation  
189 carried out using IMPUTE4.<sup>29,40,41</sup> UKB imputation involved a combination of the Haplotype  
190 Reference Consortium (HRC), the UK10K haplotype reference, and the 1000 Genomes phase 3  
191 reference panels.<sup>29</sup> To be considered a potential match for any QC-passed HCV Consortium-  
192 derived marker, the imputed UKB variant was required to have INFO score >90%, MAF >1%,

193 and HWE  $P > 1 \times 10^{-7}$ . A total of 93,095,623 imputed UKB variants met this quality control  
194 threshold and were considered for analysis.

195 Combination of the HCV Consortium and UKB datasets: Imputed markers in the HCV  
196 consortium were matched to UKB QC-passed imputed markers using position and allele  
197 information. A total of 6,025,969 markers were shared across the ancestry-matched UKB and  
198 HCV Consortium databases. A total of 6,009,835 markers were shared across the combined  
199 HCV Consortium and a set of 364,308 UKB controls who passed a more stringent set of  
200 sample-level genetic heterozygosity-focused QC metrics than those performed by the UKB  
201 consortium, as described below and in the **Supplementary Methods**.

202 Selection of different subsets of UKB population-based controls for exploratory GWAS:

203 Additional exploratory GWAS using different subsets of UKB controls were performed to  
204 determine whether the observed association between certain genetic loci and HCV clearance  
205 was driven by mismatched fine-scale ancestry, excess sample-level genetic heterozygosity, or  
206 unaccounted for population structure due to the extreme number of population-based UKB  
207 controls (**Figures S3-S8**). Other exploratory GWAS assessed differential enrichment for certain  
208 epidemiological factors relative to the population based common controls. This included a  
209 GWAS comparing the set of HCV clearance cases from non-hemophilia-focused cohorts  
210 (N=513) to a more precisely matched case-control cohort of UKB controls (N=4,908) (**Figure**  
211 **S9**). A GWAS comparing all the individuals from the HCV Consortium (N=1,739) to the  
212 European ancestry-matched population-based controls from the UKB (N=370,702) was also  
213 performed (**Figure S10**). Each exploratory GWAS occurred after performing all sample-level  
214 and imputed marker-level QC described above.

## 215 **Statistical analysis**

### 216 **HCV GWAS using cases and well characterized controls or population-based controls**

217 Association of cases and well characterized controls

218 Genetic associations between the 702 cases and 1,037 well-characterized controls of the HCV  
219 Consortium were performed via logistic regression under an additive genetic model using  
220 PLINK,<sup>32,42</sup> as the lack of any significant sample size imbalance between cases and controls or  
221 intensive computational resources needed to perform these genetic associations did not warrant  
222 a more complex association approach. Covariates for this GWAS included sex and the first  
223 twenty principal components, estimated from the HCV Consortium dataset after linkage  
224 disequilibrium-based pruning.

### 225 Association of cases and population-based controls

226 To account for the severe sample size imbalance between cases and controls, and to optimize  
227 computational performance at extreme differences in sample sizes, associations between the  
228 702 cases and 370,702 ancestry-matched population-based controls were performed under an  
229 additive genetic model using REGENIE with the saddle point approximation (SPA) test<sup>3,43,44</sup>  
230 While REGENIE partially accounts for population stratification, the top twenty PCs estimated  
231 from the combined HCV-UKB cohort were included as fixed effect covariates to ensure  
232 differences due to genetic ancestry or population structure among UKB individuals of European  
233 ancestry were accounted for (**Figure S2**).<sup>45,46</sup> Sex was included as a covariate.

234 We utilized a genome-wide significance threshold of  $P \leq 5 \times 10^{-8}$ .<sup>22</sup> After performing the  
235 association testing, to minimize the risk of bias due to differences across genotyping arrays or  
236 imputation panels between our cases and controls among putative HCV clearance-associated  
237 loci, a MAF-based filter was used to exclude markers suggestively associated with HCV  
238 clearance ( $P \leq 5 \times 10^{-5}$ ) using genome-wide allele frequency data for the gnomAD non-Finnish  
239 European population downloaded in September 2021, using the gnomAD v2.1.1 release.<sup>10</sup> Any  
240 suggestively associated marker with a  $MAF > 10\%$  among gnomAD non-Finnish Europeans was  
241 excluded if the MAF among UKB controls and gnomAD non-Finnish Europeans differed in  
242 absolute terms by at least 5%. Similarly, any suggestively associated marker with a  $MAF < 10\%$

243 in gnomAD non-Finnish Europeans was excluded if the relative difference between the  
244 gnomAD-derived MAF and UKB MAF was greater than 25%.  
245 Manhattan and quantile-quantile plots for each GWAS were generated using the ggfastman or  
246 qqman packages in R (**Figure S14**).<sup>47</sup> A table of all suggestively associated markers ( $P < 5 \times 10^{-5}$ )  
247 for the ancestry-matched UKB controls GWAS can be found within the supplemental material  
248 (**Supplementary Table 2**).

249 We performed Cochran's Q test of heterogeneity using METAL to determine whether the results  
250 obtained from the GWAS of cases vs. population-based controls from the UKB differed  
251 significantly from the GWAS of cases vs. well-characterized controls from the HCV consortium  
252 (**Figure S11**).<sup>48,49</sup>

## 253 **RESULTS**

### 254 **Simulations to characterize pathogen exposure-associated selection bias**

255 Simulations were performed using a simplified version of the framework presented in **Figure 1**.  
256 Briefly, the association between a SNP not associated with outcome but associated with  
257 pathogen exposure via the variable 'U1', was compared between pathogen exposed cases and  
258 pathogen exposed (well-characterized) or population-based common controls.

259 First, we simulated whether the presence and magnitude of the U1~'pathogen exposure'  
260 relationship affects the association between a SNP linked to U1 and the outcome of interest  
261 (**Table 1**). To provide a baseline for further explorations, the first model was simulated to have  
262 no association between U1 and pathogen exposure (OR=1). As expected, we found no  
263 association between the SNP and outcome, regardless of the choice of well-characterized or  
264 population-based controls or whether cases were compared to 20,000 population-based  
265 common controls or 200,000 population-based common controls ( $P=1$ ) (**Figure 2**). For all  
266 simulation scenarios, no replicates comparing cases and well-characterized pathogen exposed  
267 controls resulted in spurious 'outcome of interest'~SNP associations (**Table 2**).

268 For cohorts with a moderate association between U1~'pathogen exposure' (OR=1.2) there was  
269 an observed but non-significant inflation for comparisons involving 20,000 population based  
270 common controls compared to 20,000 well-characterized controls (P=0.15), based on the Z  
271 score estimate derived using the average effect estimates obtained when cases were compared  
272 to population-based or well-characterized controls. Additionally, a small number of replicates  
273 (N=159/500,000) had spurious genome-wide significant associations when cases were  
274 compared to population-based common controls. When the association between  
275 U1~'population exposure' was simulated to be stronger (OR=2), significantly inflated odds ratios  
276 were observed for comparisons involving 20,000 population-based common controls (P=5.3x10<sup>-6</sup>)  
277 **(Figure 2)**. For these simulations, 82.1% of replicates (N=410,503/500,000) had spurious  
278 associations (P<5x10<sup>-8</sup>) when cases were compared to 20,000 population-based common  
279 controls **(Table 2)**.

280 To investigate a scenario closer to current practice, we simulated unbalanced datasets with  
281 20,000 cases and 200,000 population-based controls. In these simulations the reduced variance  
282 due to increased statistical power across SNP ~'outcome of interest' estimates resulted in  
283 similarly inflated but higher proportions of spurious genome-wide significant replicates  
284 compared to replicates involving 20,000 population-based common controls for both moderate  
285 (N=1,792/500,000, P=0.11) and strong (N=499,666/500,000, P= 1.9 x 10<sup>-7</sup>) 'U1~pathogen  
286 exposure' association scenarios **(Figure 2, Table 2)**.

287 In the second set of simulations we varied the pathogen exposure prevalence from 5% to 100%  
288 to consider different infectious disease prevalence scenarios. All prevalence values except for  
289 universal exposure (100%) resulted in inflated effect estimates for comparisons involving  
290 population-based common controls when assuming either moderate (OR=1.2) or strong (OR=2)  
291 U1~pathogen exposure relationships, although only the strong exposure was significant **(Figure**  
292 **3, Figure S12)**. Using 20,000 cases vs. 200,000 population-based controls we observed

293 increased spurious associations for rare pathogen exposure prevalence (5%,  
294 N=36,815/500,000) which decreased to 0 replicates with spurious associations as the pathogen  
295 exposure approached 100% (or all exposed). This was present for both moderate and strong  
296 U1~pathogen exposure associations (**Table 2**), suggesting any observed bias was related to  
297 the differential misclassification of pathogen exposure when cases were compared to  
298 population-based controls. For comparisons involving 20,000 cases and 20,000 population-  
299 based controls, a single spurious replicate was observed for the scenario involving 100%  
300 pathogen exposure prevalence (**Table 2**).

301 We also evaluated if the number of cases altered the magnitude of any inflated effect estimates  
302 since infectious disease studies are often much smaller than other complex disease studies due  
303 to availability and collection of samples. When assuming a strong U1~pathogen exposure  
304 relationship and fixing other parameters to those utilized in the first scenario simulations, no  
305 observable difference in the mean inflation of the outcome~SNP association (OR~1.13) was  
306 observed for comparisons between varying numbers of cases: 500, 1,000, 5,000, 10,000 and  
307 20,000 and 200,000 population-based controls (**Figure S13**), suggesting that the bias exists  
308 regardless of case sample size.

### 309 **HCV GWAS using cases and well-characterized controls or population-based controls**

310 To assess the real-world consequences of differential pathogen exposure misclassification in  
311 GWAS of infectious disease, we explored the effects of control definitions using a previously-  
312 published GWAS of HCV spontaneous clearance versus persistence.<sup>25</sup> All cases and controls  
313 included within this previous GWAS were unequivocally exposed to HCV and the outcome of  
314 interest focused on a specific clinical sequela of infection, HCV clearance. We compared the  
315 results of this HCV clearance GWAS with the well-characterized (persistently HCV infected)  
316 controls to the same cases compared to population-based common controls from the UKB. The

317 GWAS comparing HCV clearance cases to persistently infected individuals replicated previously  
318 published loci.<sup>27,50–52</sup>

319 Replication of known HCV clearance-associated loci: In the GWAS using population-based UKB  
320 controls (702 cases vs. 370,702 population-based controls), the two primary HCV clearance-  
321 associated loci within the human leukocyte antigen (HLA) region (*HLA-DQB1*) and *IFNL3* locus  
322 were replicated ( $P < 5 \times 10^{-8}$ ; **Figure 4**). However, the effect sizes of these markers were biased  
323 towards the null compared to the GWAS using well-characterized controls (**Table S3**). The  
324 genome-wide significant *IFNL3* locus markers had odds ratios in the range of 0.37-0.45 when  
325 cases were compared to well-characterized controls, while there were odds ratios of 0.56-0.63  
326 for the population-based UKB controls comparison. The difference in effect size for each of  
327 these markers was significant (Cochran's Q test,  $P < 0.05$ , **Figure S11**), including the  
328 chromosome 19 marker in **Table 3**, and consistent with bias towards the null due to non-  
329 differential outcome misclassification from using population-based controls.

330 Use of population-based controls identifies previously unknown HCV clearance-associated loci:

331 In addition to the replication of known HCV clearance-associated loci, we identified two novel  
332 loci using population-based common controls. The first locus was on chromosome 4 within an  
333 intron of *syntaxin 18* (*STX18*) (rs58612183,  $MAF_{UKB} = 6.3\%$ ,  $OR = 1.93$ ,  $P = 3.01 \times 10^{-9}$ , **Figure 4**)  
334 but had a reduced OR and was not significant in the GWAS involving well-characterized  
335 controls ( $MAF_{Persistence} = 9.5\%$ ,  $OR = 1.22$ ,  $P = 0.084$ ). Interestingly, the minor allele frequency in the  
336 control groups differed but was within the European range of 6-10% as reported in ensemble  
337 showing a north-south gradient.<sup>53</sup> In the GWAS comparing all HCV European ancestry  
338 individuals from the HCV Consortium (persistence and clearance,  $N = 1,739$ ) to population-based  
339 UKB controls a genome-wide significant association was identified for this locus ( $P = 3.9 \times 10^{-10}$ )  
340 suggesting that this locus is not HCV clearance-specific but reflects any HCV infection (or  
341 membership in the HCV Consortium) compared to population controls with unknown viral

342 exposure. The signal in *STX18* remained associated with HCV clearance in additional  
343 exploratory GWAS except for the associations excluding cases known to have hemophilia and  
344 their ancestry-matched UKB controls ( $P=8.55 \times 10^{-4}$ ,  $OR=1.47$ ) (**Table 4**).

345 The second locus was on chromosome 2 within the long noncoding RNA (lncRNA) *MIR3681HG*  
346 (top marker rs10803744,  $MAF_{UKB}=12.5\%$ ,  $OR=1.57$ ,  $P=7.99 \times 10^{-8}$ ). Interestingly, the allele  
347 frequency differs between HCV clearance ( $MAF=17\%$ ) and HCV persistent ( $MAF=13\%$ )  
348 individuals ( $OR=1.42$ ,  $P=4.06 \times 10^{-4}$ ) with European general populations matching the HCV  
349 persistent (ensemble  $MAF$  11-15%).<sup>53</sup> While some of the exploratory GWAS efforts resulted in  
350 less extreme effects for the top *MIR3681HG* marker, no set of exploratory GWAS consistently  
351 eliminated this signal (**Supplementary Materials, Table S4**).

352 To determine if associations were driven by the imbalance in case:controls, we performed 1:1  
353 and 1:10 matching for each case with population-based common controls via two different  
354 commonly used matching methods (Mahalanobis distance and propensity score-based  
355 matching). While the Mahalanobis matched cohorts resulted in deflated estimates for the  
356 chromosome 2 *MIR3681HG* signal ( $OR \sim 1.44$ ,  $1.46$ , respectively) closer to the HCV clearance  
357 vs. HCV persistence GWAS than all ancestry-matched UKB controls, 1:10 matching resulted in  
358 the locus remaining suggestively associated ( $P=6.76 \times 10^{-7}$ ). The use of propensity score-based  
359 matching resulted in a further inflation in the effect estimate for the locus ( $OR \sim 1.76$ ,  $1.63$ ,  
360 respectively; **Table S4**). It is possible that local ancestry/population structure is driving this  
361 signal.

## 362 **DISCUSSION**

363 Understanding the epidemiological contexts where common controls risk the internal validity of  
364 a GWAS is necessary, especially with the availability of resources like biobanks and national  
365 cohorts.<sup>54</sup> While previous work using population-based controls has suggested non-differential  
366 misclassification of outcome can be partially compensated by increased sample sizes and



367 statistical power,<sup>2,6–8,10</sup> this current work demonstrates that for studies of infectious diseases, the  
368 comparison of cases to controls of unknown pathogen exposure can result in spurious  
369 associations.

370 The simulations show that ignoring pathogen exposure among controls can result in a more  
371 inflated effect estimate for loci associated with exposure when the prevalence of the  
372 pathogen is rare compared to when it is common. Thus, GWAS involving common controls  
373 investigating sequelae associated with endemic viruses like cytomegalovirus or Epstein-Barr  
374 virus may be less susceptible to exposure-linked selection bias since it is likely all adults have  
375 been exposed.<sup>55,56</sup> However, infectious outcomes specific to HIV, tuberculosis, or malaria need  
376 to consider whether the exposure profiles of the selected controls approximate the cases.  
377 Ideally, all controls would be evaluated and tested, but if that is not feasible on a large scale  
378 then sampling from high endemic areas or from subpopulations with increased burdens of  
379 disease could reduce the risk of spurious associations. Similarly, simulations indicate that  
380 epidemiological factors even moderately associated with pathogen exposure in a population  
381 where the pathogen of interest is rare can result in spurious genetic associations. This bias may  
382 be especially problematic for emerging pathogens like SARS-CoV-2 where certain comorbidities  
383 and demographic characteristics may be associated with SARS-CoV-2 exposure (i.e.  
384 occupation, living conditions) and the prevalence of the viral exposure depends upon changing  
385 political, social, economic, immune and viral factors.<sup>11,57</sup>

386 For example, in studies of disease severity/death due to COVID-19 involving population based  
387 common controls several associations have been observed within loci associated with risk  
388 factors for SARS-CoV-2 infection like blood type (e.g., ABO),<sup>6,58,59</sup> obesity,<sup>60</sup> alcohol use,<sup>61</sup> and  
389 non-European genetic ancestry.<sup>59,60</sup> Most notable is the ABO signal in chromosome 9, which is  
390 the most significantly associated locus for SARS-CoV-2 infection and significantly associated  
391 with both hospitalization and critical illness due to COVID-19 when using population-based

392 controls, according to the COVID-19 Host Genetics Initiative's meta-analysis results (r6  
393 release).<sup>6</sup> However, these markers fail to reach nominal statistical significance when controls  
394 are limited to non-hospitalized individuals with COVID-19 infection,<sup>6</sup> suggesting the ABO locus  
395 may not be a valid association. Loci associated with risk factors for SARS-CoV-2 could also  
396 result in spurious associations for other infectious disease-related outcomes when using  
397 common controls, as blood type is similarly associated with susceptibility to various bacterial  
398 infections and SARS,<sup>62,63</sup> obesity with influenza and pneumonia,<sup>64,65</sup> and alcohol use with  
399 contracting tuberculosis,<sup>66</sup> HIV,<sup>67</sup> and pneumonia.<sup>68</sup> However, multiple COVID-19 severity  
400 associated loci identified using population-based common controls may reflect real associations,  
401 as they were also successfully identified in GWAS limited to SARS-CoV-2 exposed controls  
402 (e.g, *LZTFL1*, *IFNAR2*).

403 Using empirical GWAS data we show that population-based common controls replicated HCV  
404 clearance-associated loci, however markers within the known gene association locus of *IFNL3*  
405 were significantly deflated (OR~0.6) as compared to the associations with pathogen exposed  
406 controls (OR~0.4), likely due to non-differential misclassification. In contrast, the novel HCV  
407 clearance association within *STX18* is likely spurious as it is attenuated after the removal of  
408 hemophiliac cases and their matched controls. Relatively rare in the general population,  
409 hemophilia is a major risk factor for HCV exposure,<sup>69,70</sup> and this association may have been  
410 driven by enrichment of hemophiliacs, or some other risk factor potentially related to the use of  
411 blood products, among cases compared to UKB controls ('U1~pathogen exposure'). *STX18* is a  
412 member of the soluble N-ethylmaleimide-sensitive factor attachment protein receptors (SNARE)  
413 protein family and involved in vesicular transport. *STX18* is not known to be associated with  
414 HCV clearance or infection and no association was observed for this locus in GWAS involving  
415 pathogen exposed controls.

416 The HCV association with lncRNA *MIR3681HG* remains unclear. The majority of previously  
417 published GWAS associations for this locus involve UKB controls,<sup>71-74</sup> with significantly  
418 associated phenotypes including height,<sup>75</sup> BMI,<sup>76</sup> and educational attainment.<sup>77</sup> Systemic  
419 differences between the UKB and the UK population have been described, with UKB  
420 participants being healthier than the general population (i.e. a 'healthy volunteer' bias) and  
421 genetic loci identified which are linked participation within the UKB.<sup>74,78-81</sup> These participation-  
422 associated loci have also been linked to educational attainment,<sup>81</sup> which altogether may explain  
423 particularly the biased associations in the *MIR3681HG* locus in our GWAS involving UKB  
424 participants given its association with BMI and educational attainment. A reported association  
425 with COVID-19 susceptibility is also noted.<sup>82</sup> Identified in a series of GWAS using cross-  
426 sectional snapshots of UKB participant data,<sup>82</sup> *MIR3681HG* reached genome-wide significance  
427 once but failed to remain significant despite increasing cases of COVID-19.<sup>82</sup>

428 Genetic studies aim to limit spurious findings by setting clear quality control measures, stringent  
429 significance thresholds, and requiring replication of findings to reduce the costly consequences  
430 of implementing translational analysis of spurious signals. These findings do not detract from  
431 the utility of GWAS involving population-based common controls, which remains an important  
432 and valuable approach to interrogate the genetic risk factors of human health and disease.  
433 Rather, we recommend that findings from infectious disease-focused association studies  
434 involving common controls be interpreted with context and caution.

435 In sum, the use of population-based common controls may be more problematic for infectious  
436 disease-focused GWAS than previously described depending on the probability of exposure to  
437 the infectious pathogen.<sup>7,8</sup> While true disease-associated loci can be identified, concerns related  
438 to selection bias, confounding, and misclassification are exacerbated by the inability to account  
439 for pathogen exposure among common controls.<sup>11</sup> Efforts to increase the selection of controls  
440 from areas with high prevalence or endemicity of disease or selection of older age participants if

441 there is known childhood exposure may ameliorate the risk of false findings. Otherwise, controls  
442 should be carefully selected and screened for pathogen exposure.

#### 443 **Declaration of interests**

444 All authors declare no competing interests.

#### 445 **Acknowledgments**

446 2R01AI148049 along with a COVID-19 supplement under the same grant number (D.L.T, P.D.,  
447 G.L.W) and Burroughs-Wellcome Fund, MD-GEM training grant (D.D.). Access and use of the  
448 UK Biobank was approved using application number 17712. G.L.W. was additionally supported  
449 by the National Human Genome Research Institute (NHGRI) grant R35HG011944.

#### 450 **Author contributions**

451 The study was designed by D.D., C.C., G.L.W., and P.D. Data collection was led by (D.L.T.,  
452 C.L.T, N.C., P.K., P.D.). Simulation was performed by D.D. Statistical analyses were designed  
453 and performed by D.D., C.C., G.L.W., and P.D. Manuscript was first drafted by D.D., C.C.,  
454 G.L.W., and P.D. All authors contributed to the final manuscript.

#### 455 **Data and code availability**

456 Access to individual-level phenotypic and genetic data from HCV extended genetics consortium  
457 individuals can be requested via dbGaP (phs000248.v1.p1). Access to individual-level data from  
458 the UKB can be requested at <https://www.ukbiobank.ac.uk>. Summary statistics for each GWAS  
459 performed can be viewed and downloaded at <https://my.locuszoom.org/> (Study name: HCV  
460 Consortium vs. UKB). Code used to perform simulation experiments, bipartite PCA-based  
461 matching, and gnomAD MAF-based variant-level filtering can be accessed at  
462 [https://github.com/dduchen/Population\\_Based\\_Controls\\_GWAS\\_ID\\_Manuscript](https://github.com/dduchen/Population_Based_Controls_GWAS_ID_Manuscript).

463 **References**

- 464 1. Visscher, P.M., Wray, N.R., Zhang, Q., Sklar, P., McCarthy, M.I., Brown, M.A., and Yang, J.  
465 (2017). 10 Years of GWAS Discovery: Biology, Function, and Translation. *Am. J. Hum. Genet.*  
466 *101*, 5–22.
- 467 2. Burton, P.R., Clayton, D.G., Cardon, L.R., Craddock, N., Deloukas, P., Duncanson, A.,  
468 Kwiatkowski, D.P., McCarthy, M.I., Ouwehand, W.H., Samani, N.J., et al. (2007). Genome-wide  
469 association study of 14,000 cases of seven common diseases and 3,000 shared controls.  
470 *Nature* *447*, 661–678.
- 471 3. Zhou, W., Nielsen, J.B., Fritsche, L.G., Dey, R., Gabrielsen, M.E., Wolford, B.N., LeFaive, J.,  
472 VandeHaar, P., Gagliano, S.A., Gifford, A., et al. (2018). Efficiently controlling for case-control  
473 imbalance and sample relatedness in large-scale genetic association studies. *Nat. Genet.* *50*,  
474 1335–1341.
- 475 4. Pan-UKB team (2020). Pan UKBB.
- 476 5. Canela-Xandri, O., Rawlik, K., and Tenesa, A. (2018). An atlas of genetic associations in UK  
477 Biobank. *Nat. Genet.* *50*, 1593–1599.
- 478 6. COVID-19 Host Genetics Initiative (2021). Mapping the human genetic architecture of  
479 COVID-19. *Nature* *600*, 472–477.
- 480 7. Mozzi, A., Pontremoli, C., and Sironi, M. (2018). Genetic susceptibility to infectious diseases:  
481 Current status and future perspectives from genome-wide approaches. *Infect. Genet. Evol.* *66*,  
482 286–307.
- 483 8. Mitchell, B.D., Fornage, M., McArdle, P.F., Cheng, Y.-C., Pulit, S.L., Wong, Q., Dave, T.,  
484 Williams, S.R., Corriveau, R., Gwinn, K., et al. (2014). Using previously genotyped controls in  
485 genome-wide association studies (GWAS): application to the Stroke Genetics Network (SiGN).

- 486 Front. Genet. 5, 1–7.
- 487 9. Wojcik, G.L., Murphy, J., Edelson, J.L., Gignoux, C.R., Ioannidis, A.G., Manning, A., Rivas,  
488 M.A., Buyske, S., and Hendricks, A.E. (2022). Opportunities and challenges for the use of  
489 common controls in sequencing studies. *Nat. Rev. Genet.* 0123456789,.
- 490 10. Pairo-Castineira, E., Clohisey, S., Klaric, L., Bretherick, A.D., Rawlik, K., Pasko, D., Walker,  
491 S., Parkinson, N., Fourman, M.H., Russell, C.D., et al. (2021). Genetic mechanisms of critical  
492 illness in COVID-19. *Nature* 591, 92–98.
- 493 11. Griffith, G.J., Morris, T.T., Tudball, M.J., Herbert, A., Mancano, G., Pike, L., Sharp, G.C.,  
494 Sterne, J., Palmer, T.M., Davey Smith, G., et al. (2020). Collider bias undermines our  
495 understanding of COVID-19 disease risk and severity. *Nat. Commun.* 11, 5749.
- 496 12. Munafò, M.R., Tilling, K., Taylor, A.E., Evans, D.M., and Davey Smith, G. (2018). Collider  
497 scope: when selection bias can substantially influence observed associations. *Int. J. Epidemiol.*  
498 47, 226–235.
- 499 13. Rosseel, Y. (2012). lavaan: An R Package for Structural Equation Modeling. *J. Stat. Softw.*  
500 48,.
- 501 14. R Core Development Team (2020). R: A language and environment for statistical  
502 computing. Vienna, Austria.
- 503 15. Yengo, L., Sidorenko, J., Kemper, K.E., Zheng, Z., Wood, A.R., Weedon, M.N., Frayling,  
504 T.M., Hirschhorn, J., Yang, J., and Visscher, P.M. (2018). Meta-analysis of genome-wide  
505 association studies for height and body mass index in ~700000 individuals of European  
506 ancestry. *Hum. Mol. Genet.* 27, 3641–3649.
- 507 16. Fesinmeyer, M.D., North, K.E., Ritchie, M.D., Lim, U., Franceschini, N., Wilkens, L.R.,  
508 Gross, M.D., Bůžková, P., Glenn, K., Quibrera, P.M., et al. (2012). Genetic Risk Factors for BMI

- 509 and Obesity in an Ethnically Diverse Population: Results From the Population Architecture  
510 Using Genomics and Epidemiology (PAGE) Study. *Obesity*.
- 511 17. Pulit, S.L., Stoneman, C., Morris, A.P., Wood, A.R., Glastonbury, C.A., Tyrrell, J., Yengo, L.,  
512 Ferreira, T., Marouli, E., Ji, Y., et al. (2019). Meta-analysis of genome-wide association studies  
513 for body fat distribution in 694 649 individuals of European ancestry. *Hum. Mol. Genet.* *28*, 166–  
514 174.
- 515 18. Shrine, N., Guyatt, A.L., Erzurumluoglu, A.M., Jackson, V.E., Hobbs, B.D., Melbourne, C.A.,  
516 Batini, C., Fawcett, K.A., Song, K., Sakornsakolpat, P., et al. (2019). New genetic signals for  
517 lung function highlight pathways and chronic obstructive pulmonary disease associations across  
518 multiple ancestries. *Nat. Genet.* *51*, 481–493.
- 519 19. Astle, W.J., Elding, H., Jiang, T., Allen, D., Ruklisa, D., Mann, A.L., Mead, D., Bouman, H.,  
520 Riveros-Mckay, F., Kostadima, M.A., et al. (2016). The Allelic Landscape of Human Blood Cell  
521 Trait Variation and Links to Common Complex Disease. *Cell* *167*, 1415-1429.e19.
- 522 20. Tsagris, M., and Papadakis, M. (2018). Taking R to its limits: 70+ tips. *PeerJ* *6*, 1–15.
- 523 21. Clogg, C.C., Petkova, E., and Haritou, A. (1995). Statistical Methods for Comparing  
524 Regression Coefficients Between Models. *Am. J. Sociol.* *100*, 1261–1293.
- 525 22. Panagiotou, O.A., and Ioannidis, J.P.A. (2012). What should the genome-wide significance  
526 threshold be? Empirical replication of borderline genetic associations. *Int. J. Epidemiol.* *41*, 273–  
527 286.
- 528 23. Balduzzi, S., Rücker, G., and Schwarzer, G. (2019). How to perform a meta-analysis with R:  
529 a practical tutorial. *Evid. Based. Ment. Health* *22*, 153–160.
- 530 24. Mitchell, R., Hemani, G., Dudding, T., Corbin, L., Harrison, S., Paternoster, L. (2019). UK  
531 Biobank Genetic Data: MRC-IEU Quality Control, version 2.

- 532 25. Vergara, C., Thio, C.L., Johnson, E., Kral, A.H., O'Brien, T.R., Goedert, J.J., Mangia, A.,  
533 Piazzolla, V., Mehta, S.H., Kirk, G.D., et al. (2019). Multi-Ancestry Genome-Wide Association  
534 Study of Spontaneous Clearance of Hepatitis C Virus. *Gastroenterology* 156, 1496-1507.e7.
- 535 26. Wojcik, G.L., Thio, C.L., Kao, W.H.L., Latanich, R., Goedert, J.J., Mehta, S.H., Kirk, G.D.,  
536 Peters, M.G., Cox, A.L., Kim, A.Y., et al. (2014). Admixture analysis of spontaneous hepatitis C  
537 virus clearance in individuals of African descent. *Genes Immun.* 15, 241–246.
- 538 27. Duggal, P., Thio, C.L., Wojcik, G.L., Goedert, J.J., Mangia, A., Latanich, R., Kim, A.Y.,  
539 Lauer, G.M., Chung, R.T., Peters, M.G., et al. (2013). Genome-Wide Association Study of  
540 Spontaneous Resolution of Hepatitis C Virus Infection: Data From Multiple Cohorts. *Ann. Intern.*  
541 *Med.* 158, 235.
- 542 28. Raj, A., Stephens, M., and Pritchard, J.K. (2014). fastSTRUCTURE: Variational Inference of  
543 Population Structure in Large SNP Data Sets. *Genetics* 197, 573–589.
- 544 29. Bycroft, C., Freeman, C., Petkova, D., Band, G., Elliott, L.T., Sharp, K., Motyer, A.,  
545 Vukcevic, D., Delaneau, O., O'Connell, J., et al. (2018). The UK Biobank resource with deep  
546 phenotyping and genomic data. *Nature* 562, 203–209.
- 547 30. Price, A.L., Weale, M.E., Patterson, N., Myers, S.R., Need, A.C., Shianna, K. V., Ge, D.,  
548 Rotter, J.I., Torres, E., Taylor, K.D., et al. (2008). Long-Range LD Can Confound Genome  
549 Scans in Admixed Populations. *Am. J. Hum. Genet.* 83, 132–135.
- 550 31. Galinsky, K.J., Bhatia, G., Loh, P.-R., Georgiev, S., Mukherjee, S., Patterson, N.J., and  
551 Price, A.L. (2016). Fast Principal-Component Analysis Reveals Convergent Evolution of ADH1B  
552 in Europe and East Asia. *Am. J. Hum. Genet.* 98, 456–472.
- 553 32. Chang, C.C., Chow, C.C., Tellier, L.C., Vattikuti, S., Purcell, S.M., and Lee, J.J. (2015).  
554 Second-generation PLINK: rising to the challenge of larger and richer datasets. *Gigascience* 4,



- 555 7.
- 556 33. Zheng, X., Levine, D., Shen, J., Gogarten, S.M., Laurie, C., and Weir, B.S. (2012). A high-  
557 performance computing toolset for relatedness and principal component analysis of SNP data.  
558 *Bioinformatics* 28, 3326–3328.
- 559 34. Bycroft, C., Freeman, C., Petkova, D., Band, G., Elliott, L.T., Sharp, K., Motyer, A.,  
560 Vukcevic, D., Delaneau, O., O’Connell, J., et al. (2017). Genome-wide genetic data on  
561 ~500,000 UK Biobank participants. *BioRxiv*.
- 562 35. UK Biobank (2015). Genotyping and Quality Control of UK Biobank, a Large-Scale,  
563 Extensively Phenotyped Prospective Resource: Information for Researchers (Interim Data  
564 Release, 2015). UK Biobank 1–27.
- 565 36. Manichaikul, A., Mychaleckyj, J.C., Rich, S.S., Daly, K., Sale, M., and Chen, W.-M. (2010).  
566 Robust relationship inference in genome-wide association studies. *Bioinformatics* 26, 2867–  
567 2873.
- 568 37. McCarthy, S., Das, S., Kretzschmar, W., Delaneau, O., Wood, A.R., Teumer, A., Kang,  
569 H.M., Fuchsberger, C., Danecek, P., Sharp, K., et al. (2016). A reference panel of 64,976  
570 haplotypes for genotype imputation. *Nat. Genet.* 48, 1279–1283.
- 571 38. Loh, P.-R., Danecek, P., Palamara, P.F., Fuchsberger, C., A Reshef, Y., K Finucane, H.,  
572 Schoenherr, S., Forer, L., McCarthy, S., Abecasis, G.R., et al. (2016). Reference-based phasing  
573 using the Haplotype Reference Consortium panel. *Nat. Genet.* 48, 1443–1448.
- 574 39. Das, S., Forer, L., Schön herr, S., Sidore, C., Locke, A.E., Kwong, A., Vrieze, S.I., Chew,  
575 E.Y., Levy, S., McGue, M., et al. (2016). Next-generation genotype imputation service and  
576 methods. *Nat. Genet.* 48, 1284–1287.
- 577 40. Howie, B., Fuchsberger, C., Stephens, M., Marchini, J., and Abecasis, G.R. (2012). Fast

- 578 and accurate genotype imputation in genome-wide association studies through pre-phasing.  
579 Nat. Genet. *44*, 955–959.
- 580 41. O’Connell, J., Sharp, K., Shrine, N., Wain, L., Hall, I., Tobin, M., Zagury, J.-F., Delaneau, O.,  
581 and Marchini, J. (2016). Haplotype estimation for biobank-scale data sets. Nat. Genet. *48*, 817–  
582 820.
- 583 42. Purcell, S., Neale, B., Todd-Brown, K., Thomas, L., Ferreira, M.A.R., Bender, D., Maller, J.,  
584 Sklar, P., De Bakker, P.I.W., Daly, M.J., et al. (2007). PLINK: A tool set for whole-genome  
585 association and population-based linkage analyses. Am. J. Hum. Genet. *81*, 559–575.
- 586 43. Butler, R.W. (2007). Saddlepoint Approximations with Applications (Cambridge: Cambridge  
587 University Press).
- 588 44. Mbatchou, J., Barnard, L., Backman, J., Marcketta, A., Kosmicki, J.A., Ziyatdinov, A.,  
589 Benner, C., O’Dushlaine, C., Barber, M., Boutkov, B., et al. (2021). Computationally efficient  
590 whole-genome regression for quantitative and binary traits. Nat. Genet. *53*, 1097–1103.
- 591 45. Galinsky, K.J., Loh, P.-R., Mallick, S., Patterson, N.J., and Price, A.L. (2016). Population  
592 Structure of UK Biobank and Ancient Eurasians Reveals Adaptation at Genes Influencing Blood  
593 Pressure. Am. J. Hum. Genet. *99*, 1130–1139.
- 594 46. Spence, J.P., and Song, Y.S. (2019). Inference and analysis of population-specific fine-  
595 scale recombination maps across 26 diverse human populations. Sci. Adv. *5*, eaaw9206.
- 596 47. D. Turner, S. (2018). qqman: an R package for visualizing GWAS results using Q-Q and  
597 manhattan plots. J. Open Source Softw. *3*, 731.
- 598 48. Willer, C.J., Li, Y., and Abecasis, G.R. (2010). METAL: fast and efficient meta-analysis of  
599 genomewide association scans. Bioinformatics *26*, 2190–2191.
- 600 49. Cochran, W.G. (1954). The Combination of Estimates from Different Experiments.

- 601 Biometrics 10, 101.
- 602 50. Rauch, A., Kutalik, Z., Descombes, P., Cai, T., Di Iulio, J., Mueller, T., Bochud, M., Battegay,  
603 M., Bernasconi, E., Borovicka, J., et al. (2010). Genetic Variation in IL28B Is Associated With  
604 Chronic Hepatitis C and Treatment Failure: A Genome-Wide Association Study.  
605 Gastroenterology 138, 1338-1345.e7.
- 606 51. Thomas, D.L., Thio, C.L., Martin, M.P., Qi, Y., Ge, D., O’hUigin, C., Kidd, J., Kidd, K.,  
607 Khakoo, S.I., Alexander, G., et al. (2009). Genetic variation in IL28B and spontaneous  
608 clearance of hepatitis C virus. Nature 461, 798–801.
- 609 52. Ge, D., Fellay, J., Thompson, A.J., Simon, J.S., Shianna, K. V., Urban, T.J., Heinzen, E.L.,  
610 Qiu, P., Bertelsen, A.H., Muir, A.J., et al. (2009). Genetic variation in IL28B predicts hepatitis C  
611 treatment-induced viral clearance. Nature 461, 399–401.
- 612 53. Cunningham, F., Allen, J.E., Allen, J., Alvarez-Jarreta, J., Amode, M.R., Armean, I.M.,  
613 Austine-Orimoloye, O., Azov, A.G., Barnes, I., Bennett, R., et al. (2022). Ensembl 2022. Nucleic  
614 Acids Res. 50, D988–D995.
- 615 54. Karlsen, T.H. (2022). Understanding COVID-19 through genome-wide association studies.  
616 Nat. Genet. 54, 368–369.
- 617 55. Tzellos, S., and Farrell, P.J. (2012). Epstein-barr virus sequence variation-biology and  
618 disease. Pathog. (Basel, Switzerland) 1, 156–174.
- 619 56. Cannon, M.J., Schmid, D.S., and Hyde, T.B. (2010). Review of cytomegalovirus  
620 seroprevalence and demographic characteristics associated with infection. Rev. Med. Virol. 20,  
621 202–213.
- 622 57. Wolff, D., Nee, S., Hickey, N.S., and Marschollek, M. (2021). Risk factors for Covid-19  
623 severity and fatality: a structured literature review. Infection 49, 15–28.

- 624 58. Zhao, J., Yang, Y., Huang, H., Li, D., Gu, D., Lu, X., Zhang, Z., Liu, L., Liu, T., Liu, Y., et al.  
625 (2021). Relationship Between the ABO Blood Group and the Coronavirus Disease 2019  
626 (COVID-19) Susceptibility. *Clin. Infect. Dis.* 73, 328–331.
- 627 59. Shelton, J.F., Shastri, A.J., Ye, C., Weldon, C.H., Filshtein-Sonmez, T., Coker, D., Symons,  
628 A., Esparza-Gordillo, J., Chubb, A., Fitch, A., et al. (2021). Trans-ancestry analysis reveals  
629 genetic and nongenetic associations with COVID-19 susceptibility and severity. *Nat. Genet.* 53,  
630 801–808.
- 631 60. Rozenfeld, Y., Beam, J., Maier, H., Haggerson, W., Boudreau, K., Carlson, J., and Medows,  
632 R. (2020). A model of disparities: risk factors associated with COVID-19 infection. *Int. J. Equity*  
633 *Health* 19, 126.
- 634 61. Kianersi, S., Ludema, C., Macy, J.T., Chen, C., and Rosenberg, M. (2022). Relationship  
635 between high-risk alcohol consumption and severe acute respiratory syndrome coronavirus 2  
636 (SARS-CoV-2) seroconversion: a prospective sero-epidemiological cohort study among  
637 American college students. *Addiction*.
- 638 62. Cooling, L. (2015). Blood Groups in Infection and Host Susceptibility. *Clin. Microbiol. Rev.*  
639 28, 801–870.
- 640 63. Guillon, P., Clément, M., Sébille, V., Rivain, J.-G., Chou, C.-F., Ruvoën-Clouet, N., and Le  
641 Pendu, J. (2008). Inhibition of the interaction between the SARS-CoV Spike protein and its  
642 cellular receptor by anti-histo-blood group antibodies. *Glycobiology* 18, 1085–1093.
- 643 64. FALAGAS, M.E., KOLETZI, P.K., BASKOUTA, E., RAFAILIDIS, P.I., DIMOPOULOS, G.,  
644 and KARAGEORGOPOULOS, D.E. (2011). Pandemic A(H1N1) 2009 influenza: review of the  
645 Southern Hemisphere experience. *Epidemiol. Infect.* 139, 27–40.
- 646 65. Nie, W., Zhang, Y., Jee, S.H., Jung, K.J., Li, B., and Xiu, Q. (2014). Obesity survival

- 647 paradox in pneumonia: a meta-analysis. *BMC Med.* 12, 61.
- 648 66. Simou, E., Britton, J., and Leonardi-Bee, J. (2018). Alcohol consumption and risk of  
649 tuberculosis: a systematic review and meta-analysis. *Int. J. Tuberc. Lung Dis.* 22, 1277–1285.
- 650 67. Rumbwere Dube, B.N., Marshall, T.P., Ryan, R.P., and Omonijo, M. (2018). Predictors of  
651 human immunodeficiency virus (HIV) infection in primary care among adults living in developed  
652 countries: a systematic review. *Syst. Rev.* 7, 82.
- 653 68. Simou, E., Britton, J., and Leonardi-Bee, J. (2018). Alcohol and the risk of pneumonia: a  
654 systematic review and meta-analysis. *BMJ Open* 8, e022344.
- 655 69. Goedert, J.J., Chen, B.E., Preiss, L., Aledort, L.M., and Rosenberg, P.S. (2007).  
656 Reconstruction of the Hepatitis C Virus Epidemic in the US Hemophilia Population, 1940-1990.  
657 *Am. J. Epidemiol.* 165, 1443–1453.
- 658 70. Berntorp, E., Fischer, K., Hart, D.P., Mancuso, M.E., Stephensen, D., Shapiro, A.D., and  
659 Blanchette, V. (2021). Haemophilia. *Nat. Rev. Dis. Prim.* 7, 45.
- 660 71. Ruth, K.S., Day, F.R., Tyrrell, J., Thompson, D.J., Wood, A.R., Mahajan, A., Beaumont,  
661 R.N., Wittemans, L., Martin, S., Busch, A.S., et al. (2020). Using human genetics to understand  
662 the disease impacts of testosterone in men and women. *Nat. Med.* 26, 252–258.
- 663 72. Saevarsdottir, S., Olafsdottir, T.A., Ivarsdottir, E. V., Halldorsson, G.H., Gunnarsdottir, K.,  
664 Sigurdsson, A., Johannesson, A., Sigurdsson, J.K., Juliusdottir, T., Lund, S.H., et al. (2020).  
665 FLT3 stop mutation increases FLT3 ligand level and risk of autoimmune thyroid disease. *Nature*  
666 584, 619–623.
- 667 73. Wu, Y., Byrne, E.M., Zheng, Z., Kemper, K.E., Yengo, L., Mallett, A.J., Yang, J., Visscher,  
668 P.M., and Wray, N.R. (2019). Genome-wide association study of medication-use and associated  
669 disease in the UK Biobank. *Nat. Commun.* 10, 1891.

- 670 74. Buniello, A., MacArthur, J.A.L., Cerezo, M., Harris, L.W., Hayhurst, J., Malangone, C.,  
671 McMahon, A., Morales, J., Mountjoy, E., Sollis, E., et al. (2019). The NHGRI-EBI GWAS  
672 Catalog of published genome-wide association studies, targeted arrays and summary statistics  
673 2019. *Nucleic Acids Res.* 47, D1005–D1012.
- 674 75. Kichaev, G., Bhatia, G., Loh, P.-R., Gazal, S., Burch, K., Freund, M.K., Schoech, A.,  
675 Pasaniuc, B., and Price, A.L. (2019). Leveraging Polygenic Functional Enrichment to Improve  
676 GWAS Power. *Am. J. Hum. Genet.* 104, 65–75.
- 677 76. Zhu, Z., Guo, Y., Shi, H., Liu, C.-L., Panganiban, R.A., Chung, W., O'Connor, L.J., Himes,  
678 B.E., Gazal, S., Hasegawa, K., et al. (2020). Shared genetic and experimental links between  
679 obesity-related traits and asthma subtypes in UK Biobank. *J. Allergy Clin. Immunol.* 145, 537–  
680 549.
- 681 77. Lee, J.J., Wedow, R., Okbay, A., Kong, E., Maghziyan, O., Zacher, M., Nguyen-Viet, T.A.,  
682 Bowers, P., Sidorenko, J., Karlsson Linnér, R., et al. (2018). Gene discovery and polygenic  
683 prediction from a genome-wide association study of educational attainment in 1.1 million  
684 individuals. *Nat. Genet.* 50, 1112–1121.
- 685 78. Fry, A., Littlejohns, T.J., Sudlow, C., Doherty, N., Adamska, L., Sprosen, T., Collins, R., and  
686 Allen, N.E. (2017). Comparison of Sociodemographic and Health-Related Characteristics of UK  
687 Biobank Participants With Those of the General Population. *Am. J. Epidemiol.* 186, 1026–1034.
- 688 79. Pirastu, N., Cordioli, M., Nandakumar, P., Mignogna, G., Abdellaoui, A., Hollis, B., Kanai,  
689 M., Rajagopal, V.M., Parolo, P.D.B., Baya, N., et al. (2021). Genetic analyses identify  
690 widespread sex-differential participation bias. *Nat. Genet.* 53, 663–671.
- 691 80. Alten, S. Van, Domingue, B.W., Galama, T., and Marees, A.T. (2022). Reweighting the UK  
692 Biobank to reflect its underlying sampling population substantially reduces pervasive selection  
693 bias due to volunteering. *MedRxiv*.

- 694 81. Tyrrell, J., Zheng, J., Beaumont, R., Hinton, K., Richardson, T.G., Wood, A.R., Davey Smith,  
695 G., Frayling, T.M., and Tilling, K. (2021). Genetic predictors of participation in optional  
696 components of UK Biobank. *Nat. Commun.* 12, 886.
- 697 82. Florian Thibord, Melissa V. Chan, Ming-Huei Chen, A.D.J. (2021). A year of Covid-19  
698 GWAS results from the GRASP portal reveals potential SARS-CoV-2 modifiers v2. MedRxiv.

## Pathogen exposure misclassification can bias association signals in GWAS of infectious diseases when using population-based common controls

### Figures and Tables

#### Figures

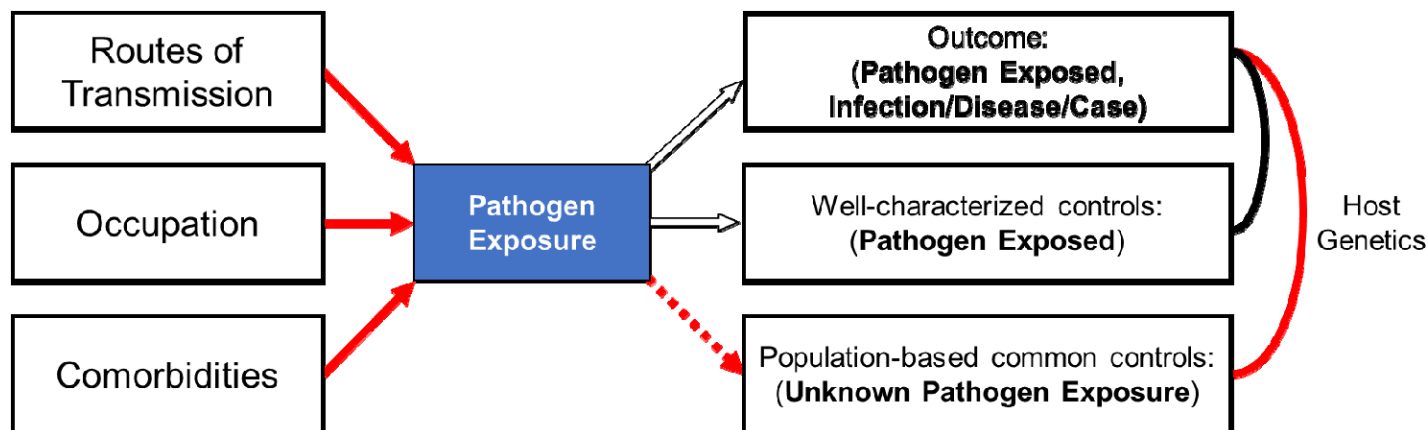
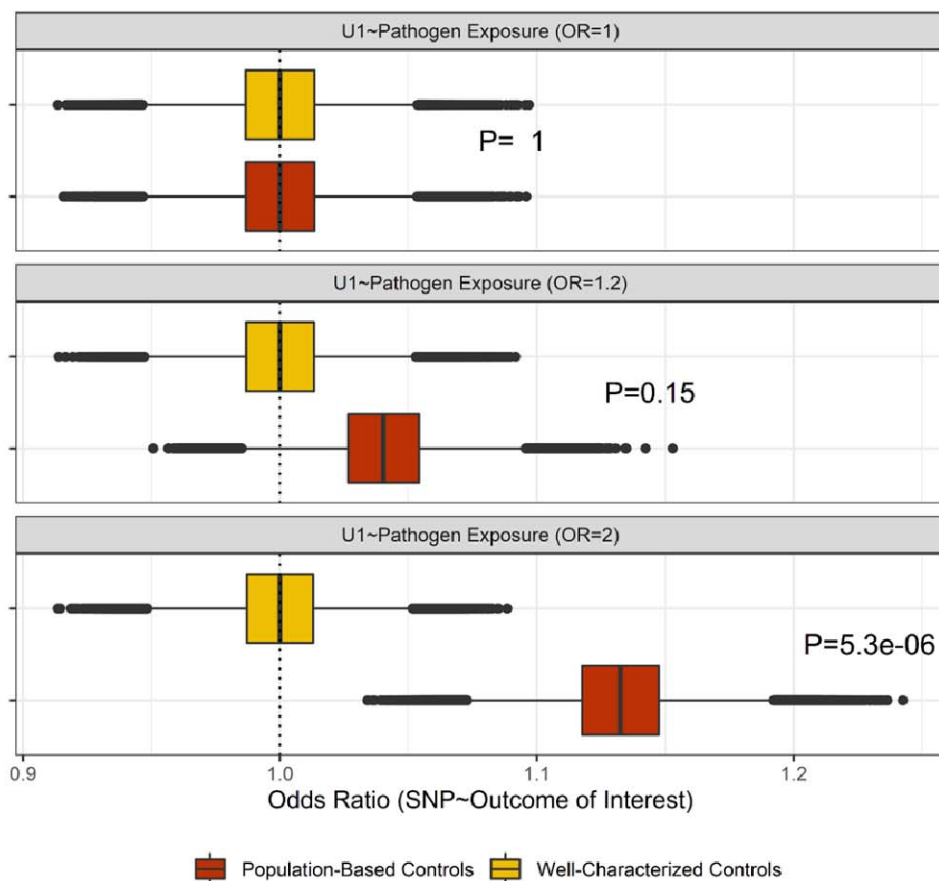


**Figure 1:** Conceptual framework of pathogen exposure-linked selection bias due to the differential misclassification of pathogen exposure and the use of population-based common controls. GWAS comparing unequivocally exposed cases to controls regardless of pathogen exposure can result in spurious (false positive) associations between loci not associated with the outcome if the loci are associated with pathogen exposure. The comparison of universally exposed cases to semi-exposed controls (host genetics, red line comparison) results in differential misclassification of pathogen exposure, introducing associations between pathogen exposure (and risk factors for pathogen exposure) and the outcome. No spurious association is expected when pathogen exposed cases are compared to pathogen exposed well-characterized controls (host genetics, black line comparison). Arrows dictate the direction of hypothesized causal effects. Hollow arrows reflect conditional relationships between exposure and outcome/case selection. The dashed arrow reflects an association induced via the differential misclassification of pathogen exposure. Red arrows highlight paths involved with pathogen exposure-linked selection bias, which results in observed associations between risk factors of pathogen exposure (and their linked loci) and an outcome of interest when cases are compared to population-based common controls of unknown pathogen exposure status.



### 20,000 Cases vs. 20,000 Population-based common controls



### 20,000 Cases vs. 200,000 Population-based common controls

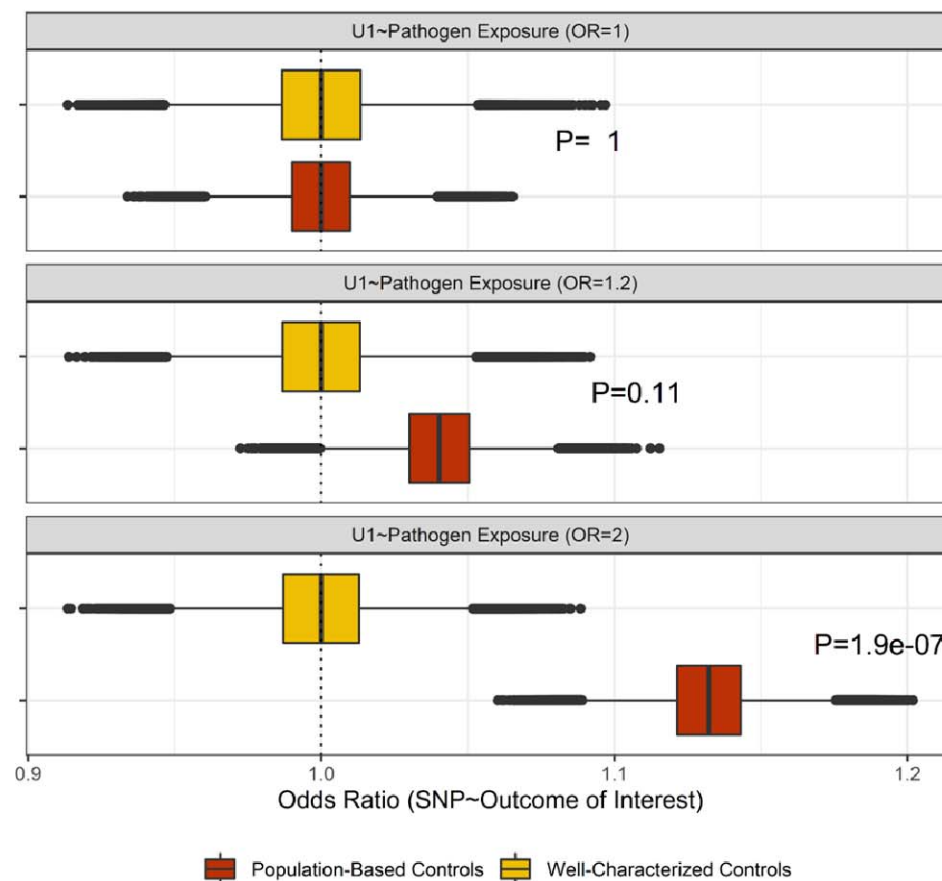


**Figure 2:** Distribution of observed odds ratios for a non-outcome associated locus across varying U1~Pathogen exposure associations. Comparisons involved 20,000 cases and equal numbers of well-characterized or population-based controls (left) or 20,000 cases and equal numbers of well-characterized and 200,000 population-based controls (right). Boxplots reflect distribution of odds ratios obtained comparing cases to population-based (red) or well-characterized controls (yellow). Reported P-values derived from a Z score based on the difference between averaged beta estimates when using population-based controls vs. well-characterized controls.

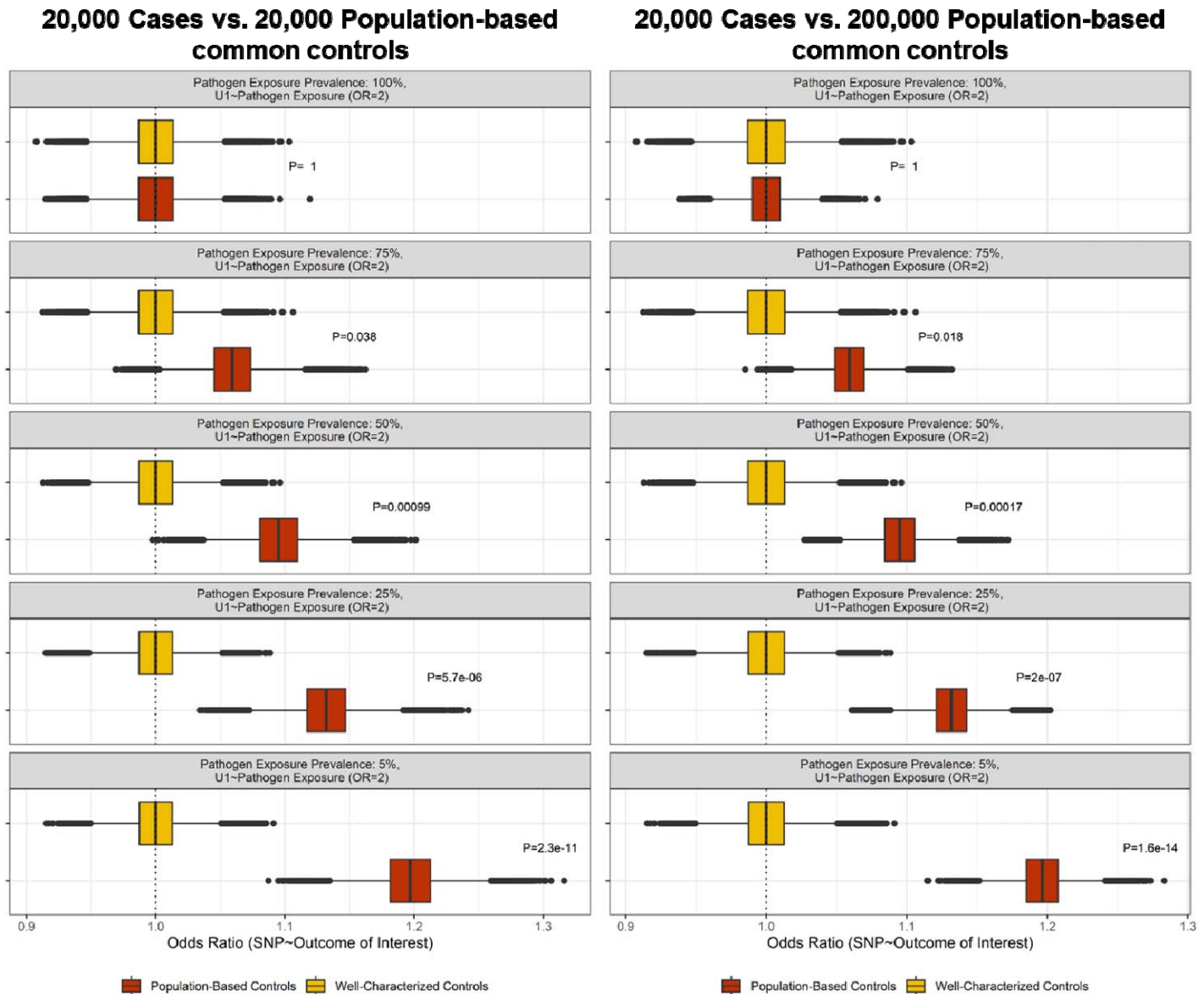


**Figure 3: Distribution of observed odds ratios for a non-outcome strongly associated locus across varying pathogen exposure prevalence.** Comparisons involved 20,000 cases and equal numbers of well-characterized or population-based controls (left) or 20,000 cases and equal numbers of well-characterized and 200,000 population-based controls (right) assuming a strong U1~'Pathogen exposure' relationship. Boxplots reflect distribution of odds ratios comparing cases to population-based (red) or well-characterized controls (yellow). Reported P-values derived from a Z score based on the difference between averaged beta estimates when using population-based controls vs. well-characterized controls.

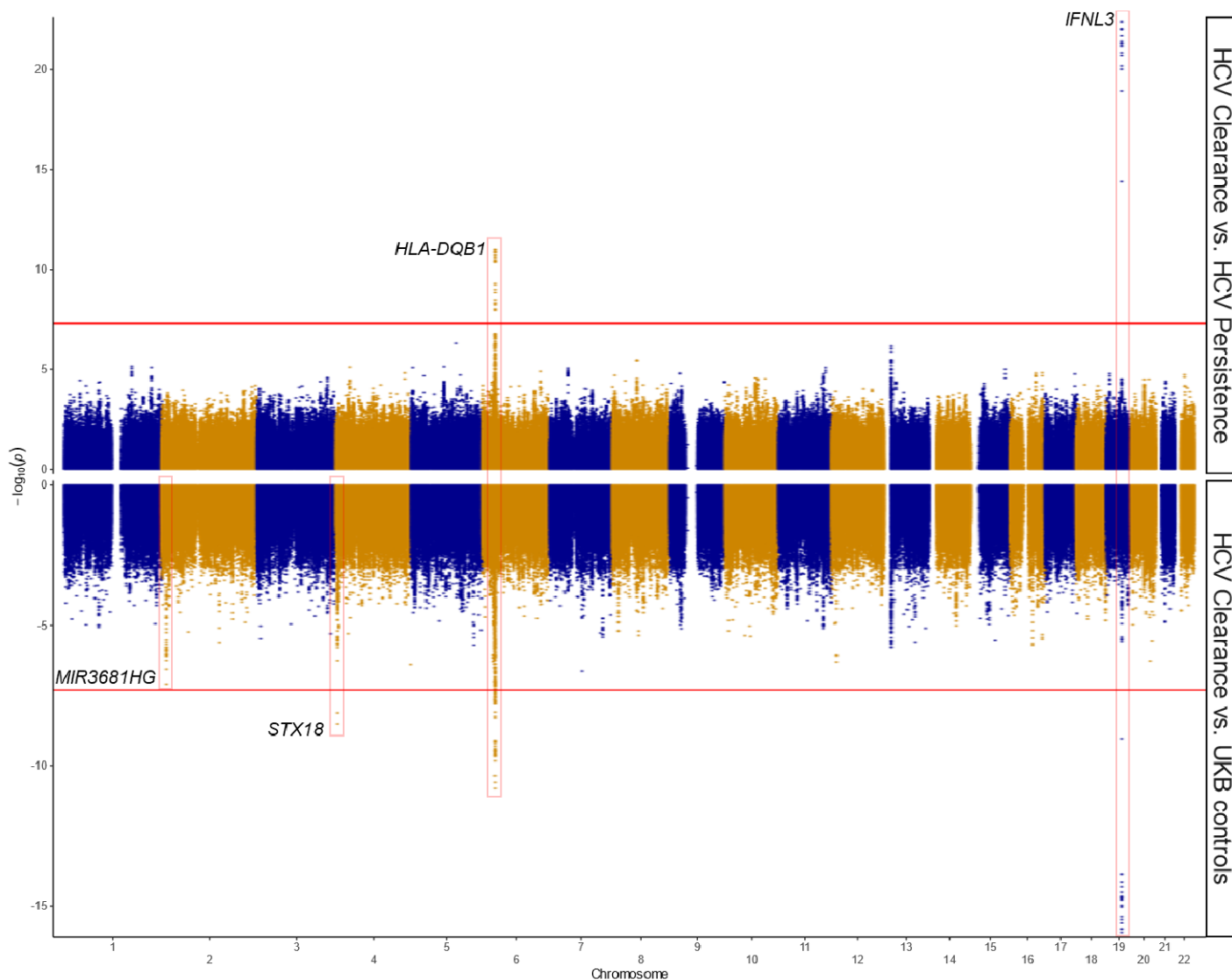


**Figure 4:** Manhattan plot of the GWAS comparing HCV clearance cases to persistently infected well-characterized controls (top) and ancestry-matched population-based UKB controls (bottom). The top panel reflects results from a GWAS performed comparing HCV clearance individuals (N=702) to individuals persistently infected with HCV from the HCV Consortium (N=1,037). The bottom panel reflects the results of a GWAS performed comparing the same HCV clearance cases to ancestry-matched population-based common controls from the UKB (N=370,702). The same set of genome-wide markers were used in each GWAS (6,025,969 markers). Points reflect the P values for each marker across the genome, ordered along the X axis by chromosomal position. The Y axis reflects the  $-\log_{10}(P)$  value, with the most significantly associated markers farthest away from 0 and outside the genome-wide significance threshold ( $P < 5 \times 10^{-8}$ ), indicated by the red lines. Loci of interest are highlighted and annotated with their nearest/overlapping gene, with novel HCV clearance-associated loci highlighted in the bottom panel.

## Tables

Simulation		Scenario-specific parameter	Fixed Values			
			Outcome: Post-exposure	Pathogen Exposure Prevalence	$\beta$ : U1~Pathogen Exposure	Sample size: Cases (N):Controls (N)
Scenario 1a: Cases vs. Population-Based Controls		$\beta$ : U1~Pathogen Exposure	50%	25%	$\log(1)$ , $\log(1.2)$ , $\log(2)$	20,000 : 20,000
Scenario 1b: Cases vs. Well-Characterized Controls						20,000 : 200,000
Scenario 2a: Cases vs. Population-Based Controls		Pathogen Exposure Prevalence	50%	5%, 25%, 50%, 75%, 100%	$\log(1.2)$ $\log(2.0)$	20,000 : 20,000
Scenario 2b: Cases vs. Well-Characterized Controls						20,000 : 200,000

**Table 1:** Simulation scenario parameters. For each scenario, the parameter of interest, the fixed values, and the sample sizes of each simulation is listed.

Scenario	Controls	Parameter Value	U1~Pathogen Exposure	20,000 Cases vs. 20,000 Common Controls		20,000 Cases vs. 200,000 Common Controls	
				OR (Mean)	Spurious Associations N (%)	OR (Mean)	Spurious Associations N (%)
1	Pathogen exposed	U1~Pathogen Exposure	OR=1	1	0	1	0
			OR=1.2	1	0	1	0
			OR=2	1	0	1	0
	Population-based	U1~Pathogen Exposure	OR=1	1	0	1	0
			OR=1.2	1.04	159 (0.03)	1.04	1,792 (0.36)
			OR=2	1.13	410,503 (82.1)	1.13	499,666 (99.93)
2	Pathogen exposed	Pathogen Exposure	OR=1.2	1	0 (0)	1	0 (0)
	Population-based			1.06	2,830 (0.57)	1.06	36,815 (7.36)
	Pathogen exposed	Prevalence: 5%	OR=2	1	0 (0)	1	0 (0)
	Population-based			1.2	499,962 (99.99)	1.197	500,000 (100)
	Pathogen exposed	Pathogen Exposure	OR=1.2	1	0 (0)	1	0 (0)
	Population-based			1.04	153 (0.03)	1.04	1,749 (0.35)
	Pathogen exposed	Prevalence: 25%	OR=2	1	0 (0)	1	0 (0)
	Population-based			1.13	407,864 (81.57)	1.132	499,647 (99.93)
	Pathogen exposed	Pathogen Exposure	OR=1.2	1	0 (0)	1	0 (0)
	Population-based			1.03	13 (<0.01)	1.03	136 (0.03)
	Pathogen exposed	Prevalence: 50%	OR=2	1	0 (0)	1	0 (0)
	Population-based			1.095	101,203 (20.24)	1.095	399,122 (79.82)
	Pathogen exposed	Pathogen Exposure	OR=1.2	1	0 (0)	1	0 (0)
	Population-based			1.019	3 (<0.01)	1.019	10 (<0.01)
	Pathogen exposed	Prevalence: 75%	OR=2	1	0 (0)	1	0 (0)
	Population-based			1.06	2,725 (0.55)	1.059	35,680 (7.14)
	Pathogen exposed	Pathogen Exposure	OR=1.2	1	0 (0)	1	0 (0)
	Population-based			1	1 (<0.01)	1	0 (0)
	Pathogen exposed	Prevalence: 100%	OR=2	1	0 (0)	1	0 (0)
	Population-based			1	1 (<0.01)	1	0 (0)

**Table 2: Proportion of spurious associations and odds ratios across scenario-specific simulated cohorts.** For each scenario, the parameter of interest, the fixed values, and the sample sizes of each simulation is listed. OR: odds ratio.

Analyzed groups	Chromosome 6 <i>HLA-DQB1</i> , rs9275241					Chromosome 19 <i>IFNL3</i> , rs11881222				
	OR	95% CI	P value	Cases (EAF, G)	Controls (EAF, G)	OR	95% CI	P value	Cases (EAF, G)	Controls (EAF, G)
Cases vs. well-characterized controls (HCV Persistence)	0.614	0.532-0.708	1.90x10 <sup>-11</sup>	39.46%	51.49%	0.424	0.358-0.503	4.06x10 <sup>-23</sup>	20.09%	36.31%
Cases vs. Ancestry-matched population-based controls (UKB)	0.691	0.620-0.772	4.35x10 <sup>-11</sup>	39.46%	52.12%	0.609	0.541-0.686	4.04x10 <sup>-16</sup>	20.09%	28.15%

**Table 3: Known HCV clearance associated loci.** Results of the association for the top HCV clearance-associated markers within the *HLA-DQB1* and *IFNL3* loci from the GWAS comparing cases with well-characterized controls from the HCV Consortium or ancestry matched population-based common UKB controls. Measures of association and frequency of the effect allele for each locus are provided for each analysis. OR: Odds Ratio. 95% CI: 95% confidence interval of the OR. EAF: Effect allele frequency.

Analyzed Groups	Chromosome 4: <i>STX18</i> , rs58612183				
	OR	95% CI	P value	Clearance (EAF, C)	Controls (EAF, C)
Cases vs. well-characterized controls (HCV Persistence)	1.22	0.97-1.54	8.40x10 <sup>-2</sup>	10.97%	9.50%
Cases vs. Ancestry-matched population-based controls (UKB)	1.93	1.56-2.41	3.01x10 <sup>-9</sup>	10.97%	6.33%
No Hemophiliacs: Cases vs. Ancestry-matched population-based controls (UKB, Matched 1:10)	1.47	1.17-1.84	8.55x10 <sup>-4</sup>	9.55%	6.65%

**Table 4:** Novel HCV clearance associated chromosome 4 locus. Results of the association for the top HCV clearance-associated marker within the *STX18* locus from the GWAS with cases vs. ancestry-matched population-based UKB controls. Measures of association and frequency of the effect allele (C) are also reported for the analysis of all cases vs all well-characterized controls GWAS and a matched case-control cohort GWAS excluding HCV clearance cases with hemophilia and their matched population-based controls. OR: Odds Ratio. 95% CI: 95% confidence interval of the OR. EAF: Effect allele frequency.